This is a preprint, the final version is subject to change, of the American Mineralogist (MSA)
Cite as Authors (Year) Title. American Mineralogist, in press.
(DOI will not work until issue is live.) DOI: http://dx.doi.org/10.2138/am-2017-5948

Revision 1

Fluorwavellite, $Al_3(PO_4)_2(OH)_2F \cdot 5H_2O$, the fluorine analogue of wavellite.

ANTHONY R. KAMPF[1*], PAUL M. ADAMS[2], HENRY BARWOOD[3§], AND BARBARA P. NASH[4]

[1]Mineral Sciences Department, Natural History Museum of Los Angeles County, 900 Exposition Boulevard, Los Angeles, CA 90007, U.S.A.

[2]126 South Helberta Avenue, #2, Redondo Beach, California 90277, U.S.A.

[3]Department of Chemistry and Physics, Troy University, 501 University Ave., Troy, Alabama 36082, U.S.A.

[4]Department of Geology and Geophysics, University of Utah, Salt Lake City, UT 84112, U.S.A.

ABSTRACT

Fluorwavellite (IMA2015-077), $Al_3(PO_4)_2(OH)_2F \cdot 5H_2O$, the F analogue of wavellite, is a new mineral from the Silver Coin mine, Valmy, Iron Point district, Humboldt County, Nevada, and the Wood mine, 5 miles NE of Del Rio, Cocke County, Tennessee; at both occurrences it is a low-temperature secondary mineral. Fluorwavellite is essentially identical to wavellite in appearance and physical properties. Optically, fluorwavellite is biaxial positive, with α =

* akampf@nhm.org
§ Deceased

1.522(1), β = 1.531(1), and γ = 1.549(1) (white light). Electron microprobe analyses (average of 9 for each cotype locality) provided the empirical formulas $Al_{2.96}(PO_4)_2(OH)_{1.98}F_{1.02}\cdot 5H_2O$ (+0.12 H) for the Silver Coin mine and $Al_{2.98}(PO_4)_2(OH)_{2.11}F_{0.89}\cdot 5H_2O$ (+0.06 H) for the Wood mine. Fluorwavellite is orthorhombic, *Pcmn*, with the cell parameters determined on a Wood mine crystal: a = 9.6311(4), b = 17.3731(12), c = 6.9946(3) Å, V = 1170.35(11) Å^3, and Z = 4. The five strongest lines in the X-ray powder diffraction pattern are [d_{obs} in Å(I)(hkl)]: 8.53(100)(020,110); 5.65(26)(101); 3.430(28)(141,012); 3.223(41)(240); and 2.580(28)(331,161,232). The structure of fluorwavellite (R_1 = 3.42% for 1248 $F_o > 4\sigma F$ reflections) is the same as that of wavellite, differing only in having one of the two independent hydroxyl sites replaced by F. A survey of F contents in wavellite-fluorwavellite from the five most common genetic types of occurrence (fluid expulsion, hydrothermal ore alteration, pegmatite phosphate alteration, residual carbonate weathering, and sedimentary leached zone) shows that F content, and the occurrence of wavellite *vs* fluorwavellite, does not correlate with the type of the occurrence. It is more likely related to the fluid activity of Al, P, and F, with pH probably being an important factor. The role that wavellite and fluorwavellite play in sequestering F in the environment may be significant.

Keywords: fluorwavellite; new mineral; crystal structure; Raman spectroscopy; Infrared spectroscopy; wavellite; Silver Coin mine, Nevada, USA; Wood mine, Tennessee, USA.

INTRODUCTION

Wavellite is a relatively common secondary mineral found in a variety of deposits. Most references (e.g. Palache et al. 1951) note that it occurs most often in aluminous, low-grade metamorphic rocks, in limonite and phosphate-rock deposits, and more rarely in hydrothermal

46 veins. Green et al. (2007) provided a synopsis of early work on the mineral. It was first
47 recognized in the early 1780s at the High Down quarry near Barnstaple, Devon (Devonshire),
48 England, and was formally described by Sir Humphry Davy in 1805 under the name hydrargillite.
49 The first reliable chemical analysis was by Jöns Jacob Berzelius and was reported by William
50 Phillips in 1823. Since then, wavellite has been found in hundreds of deposits worldwide. The
51 end-member formula is $Al_3(PO_4)_2(OH)_3 \cdot 5H_2O$ and this is the formula for the species officially
52 accepted by the International Mineralogical Association; but many references (e.g. Anthony et al.
53 2000) give the simplified formula as $Al_3(PO_4)_2(OH,F)_3 \cdot 5H_2O$ in recognition of the commonly
54 observed substitution of F for OH up to about 1 atom per formula unit (apfu).
55 Araki and Zoltai (1968) determined the structure of wavellite using a crystal from
56 Montgomery County, Arkansas. They reported two OH sites, one of 4-fold (labeled O5 here) and
57 one of 8-fold multiplicity (labeled O6 here), corresponding to one apfu and two apfu,
58 respectively. They refined both sites as O atoms, but they did not locate H sites and they did not
59 report a chemical analysis to confirm the absence of F. Capitelli et al. (2014) conducted a
60 structure refinement on a crystal from Zbirov, Czech Republic, with an analyzed F content
61 corresponding to 0.415 apfu. They located H sites related to the O5, O6, O7 and O8 sites and
62 confirmed all F to be located at the 4-fold OH site (O5), with a refined occupancy of
63 $F_{0.53(4)}O_{0.47(4)}$.
64 One of the authors (HB) has been analyzing wavellite from numerous localities for many
65 years and has confirmed F contents ranging from 0.10 to 1.02 apfu. Another author (PMA) noted
66 F contents as high as 1.03 apfu for wavellite crystals from the Silver Coin mine, Humboldt
67 County, Nevada, and 1.07 apfu for wavellite crystals from the nearby Willard mine in Pershing
68 County. These and previously published analyses (Table 1), coupled with the findings of

Capitelli et al. (2014), led us to surmise that F can fully occupy the four-fold OH site in the wavellite structure and that very little, if any, F occupies the eight-fold OH site, or any other O site in the structure. In the present study, this was confirmed by structure refinements conducted on high-F crystals from the Silver Coin mine and from the Wood mine, Cocke County, Tennessee.

In accord with the dominant-constituent rule (cf. Nickel and Grice 1998), we have proposed that wavellites containing more than ½ F apfu qualify as a distinct mineral species, the F analogue of wavellite, and that this mineral be named fluorwavellite. The new mineral and name have been approved by the Commission on New Minerals, Nomenclature, and Classification of the International Mineralogical Association (IMA2015-077). One cotype specimen from each locality is housed in the collections of the Mineral Sciences Department, Natural History Museum of Los Angeles County, 900 Exposition Boulevard, Los Angeles, California 90007, USA, catalogue numbers 65600 (Wood mine) and 65601 (Silver Coin mine).

Note that the analysis reported in Dana (1892) for wavellite from Devon, England (Table 1), which contains 0.43 F apfu, presumably corresponds to material from the wavellite type locality.

OCCURRENCE AND PARAGENESIS

Fluorwavellite occurs at many localities worldwide (see Table 1); but the complete characterization of the species is based upon material from two mines, which should be regarded as cotype localities: the Silver Coin mine, Valmy, Iron Point district, Humboldt County, Nevada (40°55'44"N 117°19'26"W) and the Wood mine, 5 miles NE of Del Rio, Cocke County,

Tennessee (35°57'52"N 82°57'36"W). At both occurrences, fluorwavellite is a low temperature, secondary mineral.

The Silver Coin mine is a small base-metal deposit that was last worked in 1929. Since the late 1980s, the mine has been a popular site for collectors in search of rare mineral species. An extensive EDS survey of wavellites from the Silver Coin mine showed all to be the new species fluorwavellite. It is found in the Phosphate Stope, Copper Stope, and Arsenate Drift. The cotype specimen is from the Copper Stope. On this specimen, fluorwavellite is associated with barite, fluorowardite, goethite, gypsum, kidwellite, quartz, and rockbridgeite. Other species observed with fluorwavellite at the Silver Coin mine are chlorargyrite, crandallite, iangreyite, jarosite, lipscombite, metavariscite, turquoise, and variscite. A comprehensive list of mineral species occurring at the Silver Coin mine is given by Adams et al. (2015). The Silver Coin mine is the type locality for zinclipscombite (Chukanov et al. 2006), meurigite-Na (Kampf et al. 2009), iangreyite (Mills et al. 2011a), krasnoite (Mills et al. 2012), fluorowardite (Kampf et al. 2014), ferribushmakinite (Kampf et al. 2015), and crimsonite (Kampf et al. 2016).

The Wood mine is a small manganese deposit that was last worked in 1906 (Stose and Schrader 1923). The ore, consisting of massive manganese oxides, mostly pyrolusite and cryptomelane, was obtained from a small open pit, which has long been overgrown. Over the last 50 years, collectors have worked the mine dumps for specimens of wavellite and variscite (Barwood 1997), which occur in veinlets in the manganese oxides.

While all of the samples from Silver Coin and Wood mines that we have analyzed qualify as fluorwavellite, the analyses listed in Table 1 clearly indicate that both wavellite and fluorwavellite occur at many deposits and that the genetic type of the deposit does not correlate

with the selective presence of either species. The occurrences of wavellite-fluorwavelite are examined in greater detail below.

PHYSICAL AND OPTICAL PROPERTIES

Fluorwavellite occurs as colorless prisms up to 1 mm long from the Silver Coin mine and up to 3 mm long from the Wood mine (Figs. 1 and 2). Crystals exhibit the forms {010}, (110}, and {101} (Fig. 3). The prisms commonly grow in radial sprays at both localities. Crystals also form bow-tie-like crystal sprays at the Silver Coin mine and dense intergrowths of subparallel prisms perpendicular to vein walls at the Wood mine. No twinning was observed.

The streak is white. Crystals are transparent with vitreous luster. The mineral does not fluoresce in long or short wave ultraviolet light. The Mohs hardness is about 3½, the tenacity is brittle, the fracture is uneven to conchoidal, and crystals exhibit three cleavages: one perfect on {110} and two good on {101} and {010}. The density of Wood mine crystals, measured by pycnometer, is 2.30(1) $g \cdot cm^{-3}$. The calculated density for Wood mine crystals based on the empirical formula and the unit cell parameters from the single-crystal data is 2.345 g/cm^3. Trapped air in crystal intergrowths could account for the somewhat low value of the measured density. Fluorwavellite is insoluble in concentrated HCl and concentrated H_2SO_4, observed over the course of several hours.

Optically, fluorwavellite is biaxial positive, with $\alpha = 1.522(1)$, $\beta = 1.531(1)$, $\gamma = 1.549(1)$, measured in white light. The $2V$ measured directly on a spindle stage is 71(1)°; the calculated $2V$ is 71.2°. Weak $r > v$ dispersion was observed. The optical orientation is X = **b**; Y = **a**; Z = **c**. The mineral is non-pleochroic.

The Gladstone-Dale compatibility index $1 - (K_P/K_C)$ as defined by Mandarino (1981) provides a measure of the consistency among the average index of refraction, unit-cell parameters (used to calculate the density) and chemical composition. For fluorowavellite, the compatibility index is -0.001 based on the empirical formula, within the range of superior compatibility.

RAMAN AND INFRARED SPECTROSCOPY

The Raman spectra of fluorwavellite from the Silver Coin and Wood mines were recorded with a Renishaw inVia microprobe using a 785 nm diode laser in order to reduce fluorescence observed with the 514 nm laser. The nominal analysis area was 5 μm x 50 μm. The Fourier transform infrared (FTIR) spectra were recorded using a Thermo Nicolet model 6700 spectrometer equipped with a Continuμm microscope. The samples were analyzed in transmission mode with a micro diamond compression cell using one diamond window as the background.

Samples from both mines yielded essentially identical results, so only the Raman and FTIR spectra for the Silver Coin samples are shown in Figures 4 and 5, respectively. Band assignments were made according to Capitelli et al. (2014). The Raman spectrum shows peaks (in cm^{-1}) at 1147, 1022 (ν_1 PO_4 symmetric stretch), 636 and 550 (ν_4 PO_4 asymmetric bend), (ν_2 PO_4), 315 and 277 (Al-O lattice vibrations). The FTIR spectrum has a sharp peak at 3521 from (OH) stretch and three broad bands at 3422, 3212, and 3092 from H_2O stretch. The H_2O bending mode was observed at 1637 and 1586 and the ν_3 (PO_4) and ν_1 (PO_4) symmetric stretch modes at 1055 and 1022, respectively. There are no significant differences between the Raman and FTIR spectra of fluorwavellite and those of F-rich wavellite reported by Capitelli et al. (2014).

This is a preprint, the final version is subject to change, of the American Mineralogist (MSA)
Cite as Authors (Year) Title. American Mineralogist, in press.
(DOI will not work until issue is live.) DOI: http://dx.doi.org/10.2138/am-2017-5948

CHEMICAL COMPOSITION

Electron probe microanalyses (EPMA; 9 spots on 3 crystals for each cotype locality) were carried out using a Cameca SX-50 electron microprobe in the Department of Geology and Geophysics at the University of Utah (WDS mode, 15 kV, 10 nA, 10 μm beam diameter). Raw X-ray intensities were corrected for matrix effects with a $\phi(\rho z)$ algorithm (Pouchou and Pichoir 1991). CHN analyses provided 22.84 wt% H_2O for material from the Wood mine; however, impurities almost certainly contribute to the lower than expected value. There was insufficient material for CHN analyses of Silver Coin material. Consequently, we have calculated H_2O for both Wood mine and Silver Coin mine analyses on the basis of P = 2 *apfu*, charge balance, and 16 O+F *apfu*, as determined by the crystal structure analysis (see below). Analytical data are given in Table 2.

The empirical formulas (based on 16 O+F) are $Al_{2.96}(PO_4)_2(OH)_{1.98}F_{1.02}\cdot 5H_2O$ (+0.12 H for charge balance) for the Silver Coin mine analyses and $Al_{2.98}(PO_4)_2(OH)_{2.11}F_{0.89}\cdot 5H_2O$ (+0.06 H for charge balance) for the Wood mine analyses. The end-member formula is $Al_3(PO_4)_2(OH)_2F\cdot 5H_2O$, which requires Al_2O_3 36.94, P_2O_5 34.29, H_2O 26.11, F 4.59, F=O -1.93, total 100 wt%.

The survey of F contents in wavellites in Table 1 includes the aforementioned analyses, other new analyses by EPMA and by scanning electron microscope wavelength dispersive spectrometry (SEM-WDS), as well as analyses reported by other investigators. The EPMA analyses were conducted on a Cameca SX-40 (15kV and 10 nA) in the Geology Department at Indiana University and the SEM-WDS analyses were conducted on a JEOL 7600F field emission SEM equipped with an Oxford WAVE WDS (10kV, 5.5 nA, and a 12 μm spot size).

X-RAY CRYSTALLOGRAPHY AND STRUCTURE REFINEMENT

Both powder and single-crystal X-ray studies were carried out using a Rigaku R-Axis Rapid II curved imaging plate microdiffractometer, with monochromatized Mo*K*α radiation. For the powder-diffraction study, a Gandolfi-like motion on the φ and ω axes was used to randomize the sample and observed *d*-values and intensities were derived by profile fitting using JADE 2010 software (Materials Data, Inc.). The powder data are presented in Table 3. Unit-cell parameters refined from the powder data using whole pattern fitting are: a = 9.6482(16), b = 17.362(3), c = 6.9848(11) Å, and V = 1170.0(3) Å^3.

Structure refinements were performed using data obtained from crystals from both the Silver Coin mine and the Wood mine. The results were very similar; however, because the refinement based on the data for the Wood mine crystal was better, it is the only one reported here. The Rigaku CrystalClear software package was used for processing of structure data, including the application of an empirical multi-scan absorption correction using ABSCOR (Higashi 2001). SHELXL-2013 software (Sheldrick 2015) was used for the refinement of the structure with neutral-atom scattering factors. The starting atom coordinates for the structure refinement were taken from the structure determination of wavellite by Capitelli et al. (2014). The O5 and O6 sites in the wavellite structure, each shared between two Al atoms, are clearly either OH or F. The occupancy of the O5(F5) site refined to $F_{0.90}O_{0.10}$, while the O6 site refined to full occupancy by O. The H atom site associated with the O6 site was located in a difference Fourier map, as were H sites associated with the O7 and O8 sites, corresponding to H_2O groups. The H sites were then refined with soft restraints of 0.82(3) Å on the O–H distances and 1.30(3) Å on the H–H distances and with the U_{eq} of each H tied to that of its O atom (×1.5 for OH and ×1.2 for H_2O). Details of data collection and structure refinement are provided in Table 4.

Fractional coordinates and atom displacement parameters are provided in Table 5, selected interatomic distances in Table 6, and bond valences in Table 7.

DESCRIPTION OF THE STRUCTURE

As for wavellite, the structure of fluorwavellite (Fig. 6) contains two different chains of corner-sharing $Al\varphi_6$ (φ = F, O, OH or H_2O) octahedra along [001]; one chain consists of all $Al1\varphi_6$ octahedra and the other of $Al2\varphi_6$ octahedra. These chains are linked to one another by corner-sharing with PO_4 tetrahedra (Fig. 7). The result is a framework structure with channels along [001]. Within these channels are disordered H_2O groups located at half-occupied O9 and O10 sites, 0.895(9) Å apart. Note that the H sites associated with these disordered H_2O groups cannot generally be located in refinements of the wavellite structure.

In the wavellite structure (and specifically in our refinement of the fluorwavellite structure), the O5/F5 and O6 sites are similar in that each is a linking corner between two $Al\varphi_6$ octahedra; O5/F5 links $Al1\varphi_6$ octahedra and the O6 site links Al2 φ_6 octahedra. The environments of these sites differ in several important respects: (1) the Al1–O5/F5 distances are much shorter than the Al2–O6 distances; (2) the chain of $Al2\varphi_6$ octahedra is significantly more kinked than the chain of $Al1\varphi_6$ octahedra (see Fig. 7) and (3) the O6 site is within reach of a potential hydrogen bond acceptor (O3 at 2.859 Å), while the closest potential hydrogen bond acceptor to O5/F5 is quite distant (O4 at 3.198 Å). (Note that the kinking of the $Al2\varphi_6$ chain facilitates the close approach of the O6 site to the O3 site.) The hydrogen bond between O6 and O3 clearly contributes to the stability of the structure and this explains why OH preferentially occupies the O6 site, and conversely why F is preferred at the O5/F5 site. In their report on the

structure refinement of an F-rich wavellite, Capitelli et al. (2014) also reported that all F is accommodated at the O5 site.

GENETIC TYPES OF WAVELLITE OCCURRENCES

Our survey of F contents in wavellites (Table 1) indicates that nearly all wavellites contain significant amounts of F and that many, if not most, are fluorwavellite. As of August 2016, there are 389 wavellite localities listed on Mindat (www.mindat.org/min-4250.html). It appears that, taken together, wavellite and fluorwavellite are the most common F-bearing phosphate minerals, outside of the apatite group, in near-surface environments. Along with members of the crandallite group, wavellite is the most common product of weathering/alteration of phosphorites and aluminous phosphatic rocks. Vast blanket deposits of both minerals exist worldwide where meteoric water leaches clay-rich phosphorites. Concentrations of wavellite have even been mined for phosphorus and aluminum salts in Pennsylvania at Moore's Mill, Cumberland County (Stose 1907; Gordon 1922) and St. Clair County, Alabama (Schrader et al. 1917).

Wavellite (including fluorwavellite) is formed in a wide variety of environments. Most reported occurrences of wavellite are of five general genetic types, which we refer to here as fluid expulsion, hydrothermal ore alteration, pegmatite phosphate alteration, residual carbonate weathering, and sedimentary leached zone. Rarer occurrences are carbonatites/syenites (four listed on Mindat) and guano deposits (one listed on Mindat). There were also 37 localities listed on Mindat that did not contain sufficient information to identify the type of occurrence.

Fluid expulsion occurrences of wavellite form in veins derived from fluid expelled during low grade metamorphism. These types of deposits are widespread and include many of the better

known locations for wavellite specimens, including the Devon, England type locality and the noteworthy wavellite occurrences in Garland, Montgomery, and Saline counties, Arkansas (Barwood and Delinde 1989). Most slate-hosted occurrences worldwide are of this type. Of the 389 localities on Mindat, 52 are of this type.

Hydrothermal ore alteration occurrences of wavellite derive from low-grade hydrothermal alteration of phosphatic rocks and alteration of apatite in ore veins (e.g. Silver Coin mine, Nevada; Llallagua, Bolivia), blanket deposits from rising volcanic solutions such as epithermal gold deposits (e.g. Carlin trend, Nevada) and acid phosphosulfate deposits (Bajnoczi et al. 2004) are common worldwide wherever they have been exposed by mining. Of the 389 localities listed on Mindat, 137 are of this type.

Pegmatite phosphate alteration occurrences of wavellite result from the alteration of aluminous primary phosphates, usually amblygonite-montebrasite, in pegmatites. Noteworthy occurrences are those at Montebras, France, and Hagendorf, Germany (Dill and Weber 2009). Of the 389 localities listed on Mindat, 19 are of this type.

Residual carbonate weathering occurrences of wavellite result from the meteoric weathering of phosphatic limestones and glauconitic sandstones and cherts, and lateritic weathering of limestone-hosted karst deposits (Hall et al. 1997; Deady et al. 2014). Widespread and numerous examples are found in old iron and manganese mines, and in bauxite deposits throughout the eastern United States (e.g. Wood mine, Tennessee) and central Europe. Of 389 localities on Mindat, 74 are of this type.

Sedimentary leached zone occurrences of wavellite derive from the meteoric weathering of phosphate-rich rocks (phosphorites) and carbonatites. Noteworthy examples of such deposits

271 are found in Florida and Senegal (Van Kauwenbergh et al. 1990; Flicoteaux and Lucas 1984). Of
272 the 389 occurrences listed on Mindat, 42 are of this type.
273 The genetic classification of all of the wavellite-fluorwavellite samples in our survey is
274 indicated in the last column of Table 1. It is clear from this survey that F content, and the
275 occurrence of wavellite *vs* fluorwavellite, does not correlate with the genetic type of the
276 occurrence. Rather, it is more likely related to the fluid activity of Al, P, and F (likely also
277 coupled with S and Fe). A noteworthy example is provided by the crystals from Slate Mountain,
278 California, examined in this study, which show zoning from F-rich cores (> 3.9% F) to F-poor
279 rims (< 0.5% F).
280

281 **THE ROLE OF pH IN THE FORMATION OF WAVELLITE AND FLUORWAVELLITE**

282 Aluminum in soils and sediments is normally highly insoluble; however, under highly
283 acidic or alkaline conditions, it forms a variety of soluble complexes. In natural waters, aquo,
284 $(OH)^-$, F^-, and organic complexes are the most important (Driscoll and Schecher 1990; Driscoll
285 et al. 2001). Using fluorescence spectroscopy, one of the authors (HB) has detected traces of
286 organic phases in wavellite. It is also well known that pH controls Al polymerization in soils
287 (Huang and Keller 1972). It is reasonable to assume that pH also plays a significant role in the
288 formation of wavellite and fluorwavellite.
289 In soils, Al has two ranges of solubility, below pH 6 and above pH 8. Under very acid
290 conditions (< pH 3), monomeric Al^{3+} is the dominant ion in solution. As the pH rises, hydrolyzed
291 OH^- complexes become more prominent. All forms of soluble Al reach a minimal solubility
292 around pH 6.5 (Driscol and Schecher 1990). Wavellite is generally insoluble in acid solutions
293 (allowing specimens to be routinely cleaned with oxalic acid and hydrochloric acid solutions). At

294 elevated pH (> 9), wavellite and fluorwavellite are readily soluble and could contribute to the
295 release of F into the environment. Such highly alkaline conditions are rare; consequently,
296 wavellite and fluorwavellite are more likely to act as sinks, rather than sources of F.

297 Fluorine in soils and sediments is invariably coupled to Al complexes. Studies have
298 shown that the maxima for soluble Al in soils also coincides with maximum absorption of F in
299 the range of pH 4.8 – 6.5 (Amesen and Krogstad 1998; Wenzel and Blum 1992). Aluminum in
300 soils and sediments is mostly associated with clay minerals and they have been shown to react
301 strongly with F. Replacement of OH in kaolinites by F has been demonstrated (Zhang et al.
302 2007), and this may have a bearing on the formation of fluorwavellite. In solution, F is entirely
303 bound by Al complexes below pH 5. As the pH rises, hydroxyl complexes of Al form, resulting
304 in more free F in solution (Skjelkvale 1994). The role of F released from apatite is not well
305 defined for any of the wavellite forming systems discussed in this paper.

306 Phosphorus in wavellite-forming systems is ultimately derived from apatite sources. The
307 phosphate anion in solution is entirely pH dependent (Tisdale et al. 1993). Reaction of phosphate
308 with Fe, Al, and Ca occurs over specific pH regions (Goldberg and Sposito 1984). Maximum
309 absorption of P by iron occurs around pH 3.5 and extends up to around pH 5.5. Phosphorus
310 sorption by aluminum begins around pH 4, peaks at around pH 5.5, and tapers off to nil around
311 pH 7. Calcium fixation begins around pH 6 and extends above pH 9. Studies of the mobility of P
312 and Al in lateritic deposits are consistent with these constraints (Huang and Keller 1972;
313 Vieillard et al. 1979). Practical observations of the sequence of mineralization in supergene Fe
314 deposits is also consistent with the sequence of pH and availability of Fe, Al, and P outlined here
315 (Dill et al. 2009).
316

IMPLICATIONS

We have noted that wavellite and fluorwavellite are formed in a wide variety of environments. Besides the reported occurrences, which mostly fall into five general genetic types (fluid expulsion, hydrothermal ore alteration, pegmatite phosphate alteration, residual carbonate weathering, and sedimentary leached zone), wavellite and fluorwavellite are widespread in soils and saprolite. Our survey of F contents shows that the occurrence of wavellite *vs* fluorwavellite, does not correlate with the genetic type of the occurrence. Coupled with our refinement of the fluorwavellite structure, we have also shown that a complete solid solution exists between wavellite and fluorwavellite and we have defined an apparent limit for the F content of wavellite-fluorwavellite of about one F *apfu*. Considering that wavellite and fluorwavellite are the most common F-bearing phosphate minerals, outside of the apatite group, in near-surface environments, our findings have implications regarding the occurrence of fluorine in the environment.

The genesis of wavellite-fluorwavellite is more complex than previously recognized. The role of P and Al availability is only partially understood and the role that hydroxyl, sulfate, organic, and fluoro Al complexes play is less well defined, but recognized. The specific fields of soluble and complexed Al, Fe, F, and P that lead to the formation of wavellite-fluorwavellite need much more study. What is well documented is that pH is clearly critical to the formation, stability and solubility of wavellite-fluorwavellite. As noted above, at elevated pH (> 9), wavellite-fluorwavellite is readily soluble and could contribute to the release of F into the environment; however, because such highly alkaline conditions are rare, wavellite-fluorwavellite is more likely to act as a sink, rather than a source of F. The role that wavellite-fluorwavellite plays in sequestering F in the environment is likely to be significant and deserves further study.

ACKNOWLEDGEMENTS

Reviewers Ferdinando Bosi and Ian Grey are thanked for their constructive comments on the manuscript. Anatoly Kasatkin is thanked for analyses of fluorwavellite samples in the collection of the Fersman Museum. A portion of this study was funded by the John Jago Trelawney Endowment to the Mineral Sciences Department of the Natural History Museum of Los Angeles County.

REFERENCES

Adams, P. M., Wise, W., and Kampf, A. R. (2015) The Silver Coin mine, Iron Point district, Humboldt County, Nevada, Mineralogical Record, 46, 701–728.

Araki, T., and Zoltai, T. (1968) The crystal structure of wavellite. Zeitschrift für Kristallographie 127, 21–33.

Arnesen, A.K.M., and Krogstad, T. (1998) Sorption and desorption of fluoride in soil polluted from the aluminum smelter at Ardal (Western Norway). Water, Air, and Soil Pollution, 103, 357–373.

Bajnóczi, B, Seres-Hartai, E., and Nagy, G. (2004) Phosphate-bearing minerals in the advanced argillic alteration zones of high-sulphidation type ore deposits in the Carpatho-Pannonian Region. Acta Mineralogica-Petrographica, Szeged, 45, 81–92.

Barwood, H. (1997) Red and pink variscite from the Wood mine, Cocke County, Tennessee. Rocks & Minerals, 72, 268–270.

Barwood, H., and Delinde, H. (1989) Arkansas phosphate minerals: a review and update. Rocks and Minerals, 64, 294–299.

363 Bergendahl, M. H. (1955) Wavellite spherulites in the Bone Valley formation of central Florida.
364 American Mineralogist, 40, 497–504.
365 Brese, N.E., and O'Keeffe, M. (1991) Bond-valence parameters for solids. Acta
366 Crystallographica, B47, 192–197.
367 Brown, I.D. and Altermatt, D. (1985) Bond-valence parameters from a systematic analysis of the
368 inorganic crystal structure database. Acta Crystallographica, B41, 244–247.
369 Capitelli, F., Della Ventura, G., Bellatreccia, F., Sodo, A., Saviano, M., Ghiara, M.R., and Rossi,
370 M. (2014) Crystal-chemical study of wavellite from Zbirov, Czech Republic. Mineralogical
371 Magazine, 78, 1057–1070.
372 Chukanov, N.V., Pekov, I.V., Möckel, S., Zadov, A.E., and V.T. Dubinchuk (2006)
373 Zinclipscombite $ZnFe^{3+}_2(PO_4)_2(OH)_2$ – a new mineral. Proceedings of the Russian
374 Mineralogical Society, 135, 13–18.
375 Dana, E.S. (1892) The System of Mineralogy of James Dwight Dana 1837-1868, 6th edition.
376 John Wiley and Sons, New York, pp. 842–843.
377 Deady, E., Mouchos, E., Goodenough, K., Williamson, B., and Wall, F. (2014) Rare earth
378 elements in karst-bauxites: a novel untapped European resource? In: ERES 2014: 1st
379 European Rare Earth Resources Conference, Milos, 4-7, September, 2014. 364–375.
380 Dill, H.G., and Weber, B. (2009) Pleystein-City on Pegmatite. 4th International Symposium on
381 Granitic Pegmatites, Recife, Brazil.
382 Dill, H.G., Weber, B., and Kaufhold, S (2009) The origin of siderite-goethite-phosphate
383 mineralization in the karst-related fault bound iron ore deposit Auerbach, Germany, a clue to
384 the timing of hypogene and supergene Fe-Al phosphates in NE Bavaria. Neues Jahrbuch für
385 Mineralogie - Abhandlungen, 186, 283–307.

386 Driscoll, C.T., and Schecher, W.D. (1990) The chemistry of aluminum in the environment.
387 Environmental Geochemical Health, 12(1), 28–49.
388 Driscoll, C.T, Lawrence, G.B., Bulger, A.J., Butler, T.J., Cronan, C.S., Eager, C., Lambert, K.F.,
389 Likens, G.E., Stoddard, J.L., and Weathers, K.C. (2001) Acidic deposition in the
390 Northeastern United States: Sources and inputs, ecosystem effects and management
391 strategies. BioScience, 51, 180–193.
392 Flicoteaux, R., and Lucas, J. (1984) Weathering of phosphate minerals. In: Phosphate Minerals,
393 J.O. Nriagu et al. (Eds). Springer-Verlag, Berlin. p. 290–317.
394 Goldberg, S., and Sposito G. (1984) A chemical model of phosphate adsorption by soils: II
395 Noncalcareous soils. Soil Science Society of America Journal, 48, 779–783.
396 Gordon, S.G. (1922) W.L. Newman mine, Pennsylvania. Mineralogy of Pennsylvania (Vol. 1). p.
397 136–138.
398 Green, D.I., Cotterell, T.F., Jones, I., Cox, D., and Cleevely, R. (2007) Wavellite: its discovery
399 and occurrences in the British Isles. UK Journal of Mines & Minerals, 28, 11–30.
400 Hall, R.B., Foord, E.E., Keller, D.J., and Keller, W.D. (1997) Phosphates in some Missouri
401 refractory clays. Clays and Clay Minerals, 45, 353–364.
402 Higashi, T. (2001) ABSCOR. Rigaku Corporation, Tokyo.
403 Huang, W.H., and Keller, W.D. (1972) Geological mechanics for the dissolution, transport and
404 deposition of aluminum in the zone of weathering. Clays and Clay Minerals, 20, 69–74.
405 Jacob, K.D., Hill, W.L., Marshall, H.L., and Reynolds, D.S. (1933) The composition and
406 distribution of phosphate rock with special reference to the United States. U.S. Department of
407 Agriculture Technical Bulletin, 364, p 40.

Kampf, A.R., Adams, P.M., Kolitsch, U. and Steele, I.M. (2009) Meurigite-Na, a new species, and the relationship between phosphofibrite and meurigite. American Mineralogist, 94, 720–727.

Kampf, A.R., Adams, P.M., Housley, R.M., and Rossman, G.R. (2014) Fluorowardite, $NaAl_3(PO_4)_2F_2(OH)_2(H_2O)_2$, the fluorine analogue of wardite from the Silver Coin mine, Valmy, Nevada. American Mineralogist, 98, 804–810.

Kampf, A.R., Adams, P.M., Nash, B.P., and Marty, J. (2015) Ferribushmakinite, $Pb_2Fe^{3+}(PO_4)(VO_4)(OH)$, the Fe^{3+} analogue of bushmakinite from the Silver Coin mine, Valmy, Nevada. Mineralogical Magazine 79, 661–669.

Kampf, A.R., Adams, P.A., Mills, S.J., and Nash, B.P. (2016) Crimsonite, $PbFe^{3+}{}_2(PO_4)_2(OH)_2$, the phosphate analogue of carminite from the Silver Coin mine, Valmy, Nevada, USA. *Mineralogical Magazine* 80, (in press, Oct. 2016)

Mäkelä, K. (1969) Wavellite from Kittilä, Finnish Lapland. Bulletin of the Geological Society of Finland, 41, 193–197.

Mandarino, J.A. (1981) The Gladstone-Dale relationship: Part IV. The compatibility concept and its application. Canadian Mineralogist, 19, 441–450.

Matsubara, S., Aito, S., and Kato, A. (1988) Phosphate minerals in chert from Toyoda, Kochi, City, Japan. Journal of Mineralogy Petrology and Economic Geology, 83, 141–149.

Mills, S.J., Kampf, A.R., Sejkora, J., Adams, P.M., Birch, W.D., and Plášil, J. (2011a) Iangreyite: a new secondary phosphate mineral closely related to perhamite. Mineralogical Magazine, 75, 329–338.

Mills, S.J., Ma, C., and Birch, W.D. (2011b) A contribution to understanding the complex nature of peisleyite. Mineralogical Magazine, 75, 2733–2737.

Mills, S.J., Sejkora, J., Kampf, A.R., Grey, I. E., Bastow, T.J., Ball, N.A., Adams, P.M., Raudsepp, M. and Cooper, M.A. (2012) Krásnoite, the fluorophosphate analogue of perhamite, from the Huber open pit, Czech Republic and the Silver Coin mine, Nevada. Mineralogical Magazine, 76, 625–634.

Nickel, E.H., Grice, J.D. (1998) The IMA Commission on New Minerals and Mineral Names: Procedures and guidelines on mineral nomenclature, 1998. Canadian Mineralogist, 36, 913–26.

Palache, C., Berman, H., and Frondel, C. (1951) Dana's System of Mineralogy, 7th edition. John Wiley and Sons, New York, Volume II, pp. 962–964.

Pouchou, J.-L., and Pichoir, F. (1991) Quantitative analysis of homogeneous or stratified microvolumes applying the model "PAP." In: Heinrich, K.F.J. and Newbury, D.E. (eds) Electron Probe Quantitation. Plenum Press, New York, pp. 3l–75.

Schrader, F.C., Stone, R.W., and Sanford, S. (1917) Useful minerals of the United States. U.S.G.S. Bulletin 624. p. 15.

Sheldrick, G.M. (2015) Crystal Structure refinement with *SHELX*. *Acta Crystallographica*, **C71**, 3–8.

Skjelkvale, B.L. (1994) Factors influencing fluoride in Norwegian lakes. Water Air Soil Pollution, 77, 151–167.

Stose, G.W. (1907) Phosphorus ore at Mt. Holly Springs, Pennsylvania. U.S.G.S. Bulletin 315, 474–483.

Stose, G.W., and Schrader, F.C. (1923) Manganese deposits of east Tennessee. U.S. Geological Survey Bulletin 737, 154 p.

453 Tisdale, S.L., Nelson, W.L., Beaton, J.D., and J.L. Havlir (1993) Influence of pH on the
454 distribution of orthophosphate species in solution. In: Soil Fertility and Fertilizers, 5th Ed.
455 MacMillan, New York, NY.
456 Van Kauwenbergh, S.J., Cathcart J.B., and McClellan, G.H. (1990) Mineralogy and alteration of
457 the phosphate deposits of Florida. U.S.G.S. Bulletin 1914, 46 pp.
458 Vieillard, P., Tardy, Y., and Nahon, D. (1979) Stability fields of clays and aluminum phosphates:
459 paragenesis in lateritic weathering of argillaceous phosphatic sediments. American
460 Mineralogist, 64, 626–634.
461 Wenzel, W.W., and Blum, W.E.H. (1992) Fluorine speciation and mobility in F-contaminated
462 soil. Soil Science, 153, 357–364.
463 Zhang, H., Baoyu, S., Penghua, L., and Wei ,Z. (2007) Experimental study of fluorine transport
464 rules in unsaturated stratified soil. Journal of China University of Mining and Technology,
465 17, 382–386.
466

FIGURE CAPTIONS

Figure 1. Fluorwavellite crystals with kidwellite from the Silver Coin mine. The FOV is 1 mm across.

Figure 2. Fluorwavellite crystals from the Wood mine. The FOV is 3.5 mm across.

Figure 3. Crystal drawing of fluorwavellite (clinographic projection).

Figure 4. Raman spectra of fluorwavellite from the Silver Coin mine.

Figure 5. FTIR spectrum of fluorwavellite from the Silver Coin mine.

Figure 6. The structure of fluorwavellite viewed along [001]. O–H bonds are thick black lines; H···O (hydrogen) bonds are thin black lines. O/F sites are numbered.

Figure 7. Two different corner-linked chains of $Al\varphi_6$ (φ = F, O, OH or H_2O) octahedra in the structure of fluorwavellite. O–H bonds are thick black lines; H···O (hydrogen) bonds are thin black lines. O/F sites are numbered.

479 Table 1. Fluorine contents of wavellite and fluorwavellite from worldwide localities.
480

Locality	**Species**	**F wt%**	**F *apfu***	**Comments**	**Genesis***
Toms quarry, Kapunda, South Australia, Australia	fluorwavellite	3.34	0.73	Mills et al. 2011b (EPMA)	S
Llallagua, Bolivia	wavellite (F-rich)	2.05	0.45	Palache et al. 1951 (wet chemistry)	H
Llallagua, Bolivia	fluorwavellite	3.34	0.73	This study (EPMA)	H
Llallagua, Bolivia	fluorwavellite	3.67	0.80	This study (EPMA)	H
Llallagua, Bolivia	fluorwavellite	4.18	0.91	This study (EPMA)	H
Llallagua, Bolivia	fluorwavellite	4.27	0.93	This study (EPMA)	H
Cerhovice, Czech Republic	wavellite	0.60	0.13	Palache et al. 1951 (wet chemistry)	H
Cerhovice, Czech Republic	fluorwavellite	4.15	0.94	A. Kasatkin pers. comm. (EPMA)	H
Svatá Dobrotivá, Czech Republic	fluorwavellite	4.34	0.98	A. Kasatkin pers. comm. (EPMA)	R
Zbirov, Czech Republic	wavellite	1.69	0.37	Dana 1892 (wet chemistry; reported as HF)	F
Zbirov, Czech Republic	wavellite (F-rich)	1.90	0.41	Capitelli et al. 2014 (EPMA)	F
Devon, England	wavellite (F-rich)	1.96	0.43	Dana 1892 (wet chemistry)	F
Devon, England	fluorwavellite	3.18	0.69	This study (SEM/WDS)	F
Kitilla, Finland	fluorwavellite (F-poor)	2.70	0.59	Mäkelä 1969 (EPMA)	H
Montebras, France	wavellite (F-rich)	2.27	0.49	Dana 1892 (wet chemistry)	P
Ronneburg, Thuringen, Germany	fluorwavellite	3.74	0.81	This study (SEM/WDS)	H
Clonmel, Ireland	fluorwavellite (F-poor)	2.79	0.61	Palache et al. 1951 (wet chemistry)	F
Cork, Ireland	wavellite (F-rich)	2.09	0.46	Dana 1892 (wet chemistry; reported as HF)	F
Toyoda, Japan	fluorwavellite	4.30	0.94	Matsubara et al. 1998 (wet chemistry)	H
Baturovskii quarry, Svetlyi, Southern Urals, Russia	fluorwavellite	3.33	0.74	A. Kasatkin pers. comm. (EPMA)	F
Baturovskii quarry, Svetlyi, Southern Urals, Russia	fluorwavellite	4.49	1.01	A. Kasatkin pers. comm. (EPMA)	F
Macadam quarry, Nikolskoe, Southern Urals, Russia	fluorwavellite	2.89	0.65	A. Kasatkin pers. comm. (EPMA)	F
Macadam quarry, Ushtaganka, Southern Urals, Russia	fluorwavellite	2.92	0.66	A. Kasatkin pers. comm. (EPMA)	F
Wavellitovaya kop', Verkhnyaya Sysert', Middle Urals, Russia	fluorwavellite	4.10	0.92	A. Kasatkin pers. comm. (EPMA)	F
Zauralovskii quarry, Zauralovo, Southern Urals, Russia	fluorwavellite	3.99	0.89	A. Kasatkin pers. comm. (EPMA)	F
Tharsis mine, Hvelva Prov., Spain	fluorwavellite	4.17	0.91	This study (EPMA)	H
Augusta Ridge, Cherokee Co., Alabama, USA	fluorwavellite	4.19	0.91	This study (EPMA)	R
SE of Weogufka, Coosa Co., Alabama, USA	wavellite	1.22	0.27	This study (EPMA)	F
SE of Weogufka, Coosa Co., Alabama, USA	wavellite	1.57	0.34	This study (EPMA)	F
SE of Weogufka, Coosa Co., Alabama, USA	wavellite (F-rich)	2.01	0.44	This study (EPMA)	F
SE of Weogufka, Coosa Co., Alabama, USA	fluorwavellite	3.23	0.70	This study (EPMA)	F
Erin, Clay Co., Alabama, USA	wavellite	0.61	0.13	This study (EPMA)	F

Erin, Clay Co., Alabama, USA	wavellite	0.78	0.17	This study (EPMA)	F
Erin, Clay Co., Alabama, USA	fluorwavellite (F-poor)	2.88	0.63	This study (EPMA)	F
Nesbit Lake, Calhoun Co., Alabama, USA	wavellite	1.34	0.29	This study (EPMA)	R
Sid Hart mine, Indian Mt., Cherokee Co., Alabama, USA	fluorwavellite	4.01	0.87	This study (EPMA)	R
East of Coal City, St. Clair Co., Alabama, USA	wavellite	0.45	0.10	This study (EPMA)	R
East of Coal City, St. Clair Co., Alabama, USA	wavellite	0.45	0.10	This study (EPMA)	R
East of Coal City, St. Clair Co., Alabama, USA	wavellite	0.48	0.10	This study (EPMA)	R
East of Coal City, St. Clair Co., Alabama, USA	wavellite (F-rich)	1.47	0.32	This study (EPMA)	R
East of Coal City, St. Clair Co., Alabama, USA	wavellite (F-rich)	1.60	0.35	This study (EPMA)	R
East of Coal City, St. Clair Co., Alabama, USA	fluorwavellite (F-poor)	2.52	0.55	This study (EPMA)	R
East of Coal City, St. Clair Co., Alabama, USA	fluorwavellite (F-poor)	2.95	0.64	This study (EPMA)	R
Dug Hill (roadcut), Garland Co., Arkansas, USA	fluorwavellite (F-poor)	2.53	0.55	This study (EPMA)	F
Dug Hill (roadcut), Garland Co., Arkansas, USA	fluorwavellite	3.60	0.78	This study (EPMA)	F
Dug Hill (roadcut), Garland Co., Arkansas, USA	fluorwavellite	3.83	0.83	This study (EPMA)	F
Dug Hill (roadcut), Garland Co., Arkansas, USA	fluorwavellite	4.07	0.89	This study (EPMA)	F
Mauldin Mt., Montgomery Co., Arkansas, USA	wavellite	0.97	0.21	This study (EPMA)	F
Mauldin Mt., Montgomery Co., Arkansas, USA	fluorwavellite (F-poor)	2.86	0.62	This study (EPMA)	F
Mauldin Mt., Montgomery Co., Arkansas, USA	fluorwavellite	3.42	0.75	This study (EPMA)	F
Polk Co., Arkansas, USA	fluorwavellite	4.08	0.89	This study (EPMA)	F
Saline Co., Arkansas, USA	wavellite	1.03	0.22	This study (EPMA)	F
Saline Co., Arkansas, USA	fluorwavellite	3.13	0.68	This study (EPMA)	F
Saline Co., Arkansas, USA	fluorwavellite	4.05	0.88	This study (EPMA)	F
Saline Co., Arkansas, USA	fluorwavellite	4.09	0.89	This study (EPMA)	F
Saline Co., Arkansas, USA	fluorwavellite	4.20	0.92	This study (EPMA)	F
Saline Co., Arkansas, USA	fluorwavellite	4.45	0.97	This study (EPMA)	F
Saline Co., Arkansas, USA	fluorwavellite	4.66	1.02	This study (EPMA)	F
Slate Mt., El Dorado Co., California, USA	wavellite	0.38	0.08	This study (EPMA; rim)	F
Slate Mt., El Dorado Co., California, USA	wavellite	0.49	0.11	This study (EPMA; rim)	F
Slate Mt., El Dorado Co., California, USA	fluorwavellite	3.89	0.85	This study (EPMA; core)	F
Clear Spring mine, Polk Co., Florida, USA	fluorwavellite	4.17	0.91	This study (EPMA)	S
Polk Co., Florida , USA	wavellite	0.93	0.20	Bergendahl 1955 (wet chemistry)	S
Brewer mine, Polk Co., Georgia, USA	fluorwavellite	3.42	0.75	This study (EPMA)	R
Kreamer, Snyder Co., Pennsylvania, USA	fluorwavellite	4.14	0.90	This study (EPMA)	R
Moore's Mill, Cumberland Co., Pennsylvania, USA	wavellite	0.69	0.15	This study (EPMA)	R
Mt. Holly Springs, Cumberland Co., Pennsylvania, USA	wavellite	0.69	0.15	This study (EPMA)	R
Mt. Holly Springs, Cumberland Co., Pennsylvania, USA	fluorwavellite	3.95	0.86	Jacob et al. 1933 (wet chemistry)	R
Wharton mine, Pennsylvania, USA	fluorwavellite	3.18	0.69	This study (EPMA)	R
Silver Coin mine, Arsenate Drift, Humboldt Co., Nevada, USA	fluorwavellite	3.65	0.80	This study (SEM/WDS)	H
Silver Coin mine, Copper Stope, Humboldt Co., Nevada, USA	fluorwavellite	4.11	0.90	This study (SEM/WDS)	H

Silver Coin mine, Copper Stope, Humboldt Co., Nevada, USA	fluorwavellite	4.74	1.03	This study (EPMA; Table 1)	H
Silver Coin mine, Phosphate Stope, Humboldt Co., Nevada, USA	fluorwavellite	3.90	0.85	This study (EPMA)	H
Willard mine, Pershing Co., Nevada, USA	fluorwavellite	4.91	1.07	This study (SEM/WDS)	H
Northern Belle mine, Candelaria, Mineral Co., Nevada, USA	fluorwavellite	3.10	0.68	This study (SEM/WDS; core)	H
Northern Belle mine, Candelaria, Mineral Co., Nevada, USA	fluorwavellite	4.07	0.89	This study (SEM/WDS; rim)	H
Copper Knob, Cocke Co., Tennessee, USA	fluorwavellite (F-poor)	2.96	0.64	This study (EPMA)	R
Wood mine, Cocke Co., Tennessee, USA	fluorwavellite	4.08	0.89	This study (EPMA; Table 1)	R
Wood mine, Cocke Co., Tennessee, USA	fluorwavellite	4.18	0.91	This study (EPMA)	R
Bingham Canyon mine, Salt Lake Co., Utah, USA	fluorwavellite	3.19	0.69	This study (EPMA)	H
Kelly Bank mine, Rockbridge Co., Virginia, USA	wavellite (F-rich)	2.14	0.47	This study (EPMA)	R
Kelly Bank mine, Rockbridge Co., Virginia, USA	fluorwavellite	3.17	0.69	This study (EPMA)	R
Rorer mine, Roanoke, Virginia, USA	fluorwavellite (F-poor)	3.02	0.66	This study (EPMA)	R

481 * Wavellite genesis types: F = Fluid expulsion, H = Hydrothermal ore alteration, P = Pegmatite phosphate alteration, R = Residual carbonate weathering, S =
482 Sedimentary leached zone

Table 2. Analytical data (wt%) for fluorwavellite.

Const.	Silver Coin mine			Wood mine			Probe Standard
	Mean	Range	SD	Mean	Range	SD	
Al_2O_3	36.79	36.35–37.07	0.22	36.68	36.42–37.09	0.21	sanidine
P_2O_5	34.66	33.90–35.51	0.50	34.31	33.50–34.95	0.42	apatite
F	4.74	4.48–4.96	0.17	4.08	3.58–4.46	0.26	syn. CaF_2
H_2O*	26.65			26.52			
F=O	-2.00			-1.72			
Total	100.84			99.87			

*Based on the structure

Table 3. Powder X-ray diffraction data (d in Å) for fluorwavellite.

I_{obs}	d_{obs}	d_{calc}	I_{calc}	hkl
100	8.53	8.6865	52	0 2 0
		8.4233	48	1 1 0
26	5.65	5.6595	26	1 0 1
10	5.39	5.3812	7	1 1 1
4	4.98	4.9630	7	1 3 0
17	4.81	4.8156	9	2 0 0
		4.7419	3	1 2 1
4	4.335	4.3433	1	0 4 0
8	4.023	4.0476	5	1 3 1
		3.9664	4	2 0 1
6	3.892	3.8669	2	2 1 1
28	3.430	3.4456	6	1 4 1
		3.4285	22	0 1 2
		3.2873	1	1 0 2
		3.2724	3	2 3 1
		3.2300	1	1 1 2
41	3.223	3.2252	27	2 4 0
		3.1569	3	3 1 0
11	3.071	3.0745	8	1 2 2
		2.9937	2	0 3 2
15	2.934	2.9611	4	1 5 1
		2.9289	4	2 4 1
		2.9177	1	3 0 1
		2.8955	2	0 6 0
		2.8774	2	3 1 1
13	2.804	2.8078	7	3 3 0
		2.7659	1	3 2 1
		2.7240	1	0 4 2
		2.6212	1	1 4 2
		2.6136	2	2 5 1
28	2.580	2.6057	4	3 3 1
		2.5777	14	1 6 1
		2.5425	4	2 3 2
4	2.476	2.4815	1	2 6 0
		2.4649	1	0 5 2
		2.4220	1	3 4 1
1	2.410	2.4078	2	4 0 0
9	2.364	2.3650	5	3 0 2
6	2.274	2.2767	4	4 0 1
		2.2729	1	1 7 1
3	2.234	2.2344	2	3 5 1
		2.2303	1	0 6 2
5	2.187	2.2023	1	4 2 1
		2.1927	1	1 2 3
		2.1728	1	1 6 2
16	2.101	2.1103	2	1 3 3
		2.1058	6	4 4 0
		2.1039	1	2 7 1
		2.0985	4	2 0 3
		2.0834	2	2 1 3
10	2.041	2.0552	2	3 6 1
		2.0398	2	2 2 3
		2.0275	1	1 8 1
		2.0240	1	0 7 2
		1.9807	1	1 7 2
15	1.9699	1.9796	5	2 8 0
		1.9635	5	3 7 0
		1.9551	1	3 5 2
		1.9145	1	5 1 0
6	1.8928	1.9043	1	4 5 1
		1.8927	1	1 9 0
		1.8905	1	3 7 1
		1.8659	1	2 7 2
		1.8435	1	3 2 3
5	1.8274	1.8317	2	3 6 2
		1.8161	1	5 2 1
		1.7684	1	5 3 1
5	1.7440	1.7487	4	0 0 4
		1.7303	1	3 4 3
8	1.7153	1.7224	4	4 5 2
		1.7121	3	1 1 4
		1.7075	1	5 4 1
5	1.6708	1.6749	1	4 0 3
		1.6735	2	1 7 3
		1.6608	1	1 10 1
2	1.6432	1.6493	1	1 3 4
		1.6447	1	4 2 3
		1.6436	1	2 0 4
		1.6221	1	0 4 4
9	1.6040	1.6126	3	4 8 0
		1.6099	1	3 9 1
		1.6052	1	6 0 0
		1.5947	3	2 9 2
		1.5812	1	2 3 4
8	1.5698	1.5727	3	5 4 2
2	1.5567	1.5586	4	1 11 0
11	1.5327	1.5372	5	2 4 4
		1.5217	2	5 7 0
3	1.4802	1.4843	2	3 3 4
		1.4723	1	4 9 1
		1.4695	1	1 9 3
9	1.4547	1.4578	5	5 6 2
		1.4537	1	6 1 2
		1.4478	2	0 12 0
7	1.4093	1.4172	1	3 11 0
		1.4147	1	6 3 2
		1.4140	2	1 7 4
		1.4026	1	1 12 1
		1.4001	1	3 10 2
3	1.3823	1.3844	1	1 0 5
		1.3833	1	4 9 2
6	1.3449	1.3500	1	7 0 1
		1.3492	1	3 9 3
		1.3486	1	1 8 4
		1.3459	1	7 1 1
		1.3453	2	4 4 4
		1.3386	1	7 3 0
6	1.3127	1.3221	1	6 0 3
		1.3147	1	7 3 1
		1.3106	1	2 8 4

Table 4. Data collection and structure refinement details for fluorwavellite from the Wood mine.*

Diffractometer	Rigaku R-Axis Rapid II
X-ray radiation / power	Mo$K\alpha$ (λ = 0.71075 Å) / 50 kV, 40 mA
Temperature	293(2) K
Structural Formula	$Al_3(PO_4)_2(OH)_2[F_{0.90}(OH)_{0.10}]\cdot 5H_2O$
Space group	*Pcmn*
Unit cell parameters	a = 9.6311(4) Å
	b = 17.3731(12) Å
	c = 6.9946(3) Å
V	1170.35(11) Å^3
Z	4
Density (for above formula)	2.353 g·cm^{-3}
Absorption coefficient	0.701 mm^{-1}
F(000)	843.6
Crystal size	130 × 75 × 45 μm
θ range	3.60 to 27.49°
Index ranges	$-12 \le h \le 12$, $-22 \le k \le 22$, $-9 \le l \le 6$
Reflections collected / unique	6066 / 1376 [R_{int} = 0.035]
Reflections with $F_o > 4\sigma F$	1248
Completeness to θ = 27.49°	99.3%
Min. and max. transmission	0.914 and 0.969
Refinement method	Full-matrix least-squares on F^2
Parameters refined / restraints	124 / 7
GoF	1.082
R indices [$F_o > 4\sigma F$]	R_1 = 0.0342, wR_2 = 0.0946
R indices (all data)	R_1 = 0.0370, wR_2 = 0.0970
Largest diff. peak / hole	+0.66 / –0.44 e/A^3

*$R_{int} = \Sigma|F_o^2\text{-}F_o^2(\text{mean})|/\Sigma[F_o^2]$. GoF = $S = \{\Sigma[w(F_o^2-F_c^2)^2]/(n-p)\}^{1/2}$. $R_1 = \Sigma||F_o|\text{-}|F_c||/\Sigma|F_o|$. $wR_2 = \{\Sigma[w(F_o^2-F_c^2)^2]/\Sigma[w(F_o^2)^2]\}^{1/2}$. $w = 1/[\sigma^2(F_o^2) + (aP)^2 + bP]$ where a is 0.0716, b is 0.1059 and P is $[2F_c^2 + \text{Max}(F_o^2,0)]/3$.

Table 5. Atom coordinates and displacement parameters (Å^2) for fluorwavellite.

	x/*a*	*y*/*b*	*z*/*c*	U_{eq}	U^{11}	U^{22}	U^{33}	U^{23}	U^{13}	U^{12}
Al1	0.22360(8)	0.25	0.12424(10)	0.0108(2)	0.0126(4)	0.0105(4)	0.0093(4)	0	-0.0004(3)	0
Al2	0.75614(5)	0.01608(3)	0.14135(7)	0.00850(18)	0.0090(3)	0.0102(3)	0.0064(3)	0.00031(17)	0.00018(19)	-0.00012(18)
P1	0.06047(4)	0.09249(2)	0.10416(6)	0.00804(18)	0.0083(3)	0.0083(3)	0.0076(3)	-0.00026(13)	-0.00008(15)	-0.00016(15)
O1	0.90414(12)	0.08341(7)	0.06432(18)	0.0110(3)	0.0091(6)	0.0140(6)	0.0099(6)	0.0015(5)	-0.0017(5)	-0.0012(4)
O2	0.08825(13)	0.17679(7)	0.15583(19)	0.0148(3)	0.0159(6)	0.0103(6)	0.0183(7)	-0.0041(5)	0.0045(5)	-0.0031(5)
O3	0.10072(12)	0.04175(7)	0.27410(18)	0.0129(3)	0.0115(6)	0.0173(6)	0.0099(6)	0.0036(5)	0.0011(5)	0.0032(5)
O4	0.35889(13)	0.07249(7)	0.42095(17)	0.0108(3)	0.0126(6)	0.0117(5)	0.0080(6)	0.0004(4)	-0.0016(5)	-0.0014(5)
F5	0.27950(19)	0.25	0.3695(2)	0.0197(6)	0.0246(10)	0.0243(10)	0.0101(9)	0	-0.0043(6)	0
O6	0.82046(14)	0.01765(7)	0.39498(16)	0.0106(5)	0.0067(7)	0.0176(7)	0.0075(7)	0.0000(4)	0.0008(4)	-0.0008(5)
H6	0.905(2)	0.0253(14)	0.398(3)	0.016						
O7	0.36874(15)	0.17072(9)	0.0972(2)	0.0228(3)	0.0213(7)	0.0241(7)	0.0230(8)	-0.0042(5)	-0.0021(6)	0.0052(6)
H71	0.372(3)	0.1362(13)	0.198(3)	0.027						
H72	0.379(3)	0.1436(14)	0.008(3)	0.027						
O8	0.65089(14)	0.11053(8)	0.1977(2)	0.0151(3)	0.0181(7)	0.0156(6)	0.0115(6)	0.0022(5)	0.0035(5)	0.0025(5)
H81	0.640(3)	0.1065(13)	0.309(3)	0.018						
H82	0.689(2)	0.1507(12)	0.173(3)	0.018						
O9	0.8088(8)	0.25	0.229(3)	0.053(4)	0.037(3)	0.036(3)	0.086(12)	0	0.015(4)	0
O10	0.7814(14)	0.25	0.107(3)	0.057(4)	0.077(6)	0.025(3)	0.069(10)	0	0.028(6)	0
Refined occupancies: F5/O5 = 0.90/0.10(5); O6/F6 = 1.00/0.00(3); O9/O10 = 0.49/0.51(3)										

Table 6. Selected bond distances (Å) in fluorwavellite.

Al1–F5	1.7818(17)	Al2–OH6	1.8747(12)	P1–O3	1.5297(12)
Al1–F5	1.7982(16)	Al2–OH6	1.8793(12)	P1–O2	1.5321(12)
Al1–O2 (×2)	1.8346(13)	Al2–O4	1.8807(13)	P1–O4	1.5382(12)
Al1–O7 (×2)	1.9715(15)	Al2–O3	1.8973(12)	P1–O1	1.5393(12)
< Al1–O>	1.8654	Al2–O1	1.9210(13)	< P1–O>	1.5348
		Al2–O8	1.9686(14)		
		< Al2–O>	1.9036		

Hydrogen bonds

D–H···*A*	*D*–H	H···*A*	*D*···*A*	<*D*–H–*A*
O6–H6···O3	0.83(2)	2.09(2)	2.8594(17)	154.3(19)
O7–H71···O4	0.92(2)	1.92(2)	2.837(2)	172(2)
O7–H72···O2	0.79(2)	2.55(2)	3.117(2)	130(2)
O7–H72···O3	0.79(2)	2.42(2)	3.1959(19)	170(2)
O8–H81···O1	0.79(2)	1.88(2)	2.6604(19)	171(2)
O8–H82···O9	0.807(19)	2.11(2)	2.869(5)	156(2)
O8–H82···O10	0.807(19)	2.00(2)	2.803(4)	179(2)

566 Table 7. Bond-valence analysis for fluorwavellite.* Values are expressed in valence units.
567

	O1	O2	O3	O4	F5	O6	O7	O8	Σ
Al1		0.60 ×2→			0.53 0.50		0.41 ×2→		3.05
Al2	0.47		0.50	0.53		0.54 0.53		0.42	2.99
P	1.23	1.26	1.27	1.24					5.00
H6			0.16						
H71				0.17			0.83		
H72		0.04					0.96		
H81	0.22							0.78	
H82								0.82	
Σ	1.92	1.90	1.93	1.94	1.03	1.07	2.20	2.02	

568 * Multiplicity is indicated by ×2→. Al–O bond valence parameter is from Brese and O'Keeffe
569 (1991) and those for P^{5+}–O and Al–F are from Brown and Altermatt (1985). Hydrogen-bond
570 strengths are based on O···O bond lengths, from Brown and Altermatt (1985). The O9 and O10
571 sites are not included.

Figure 1

Figure 2

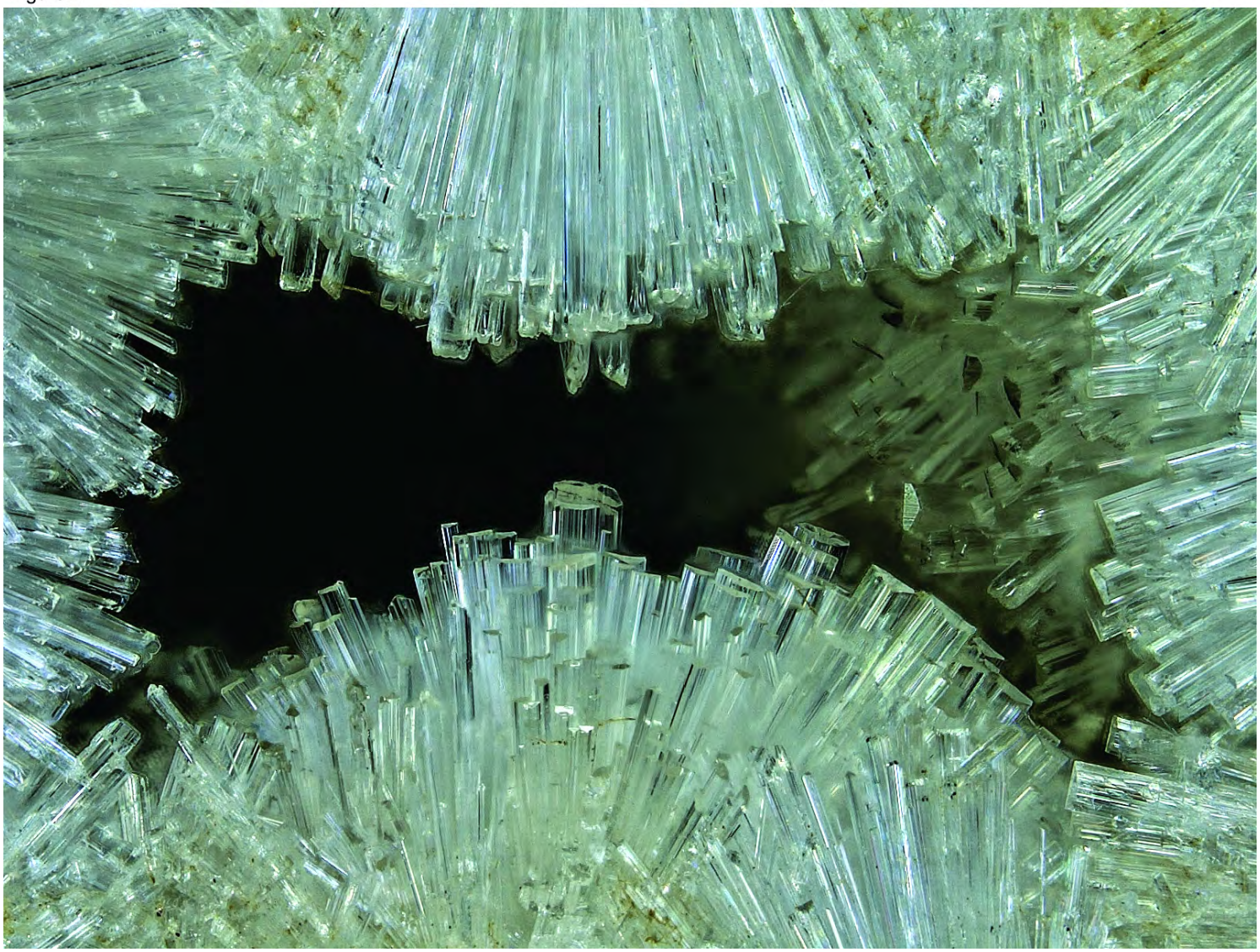

Figure 3

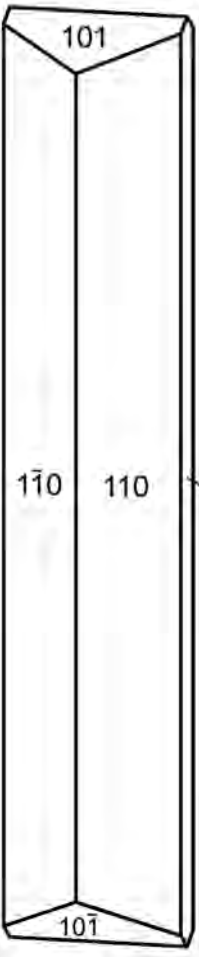

Figure 4

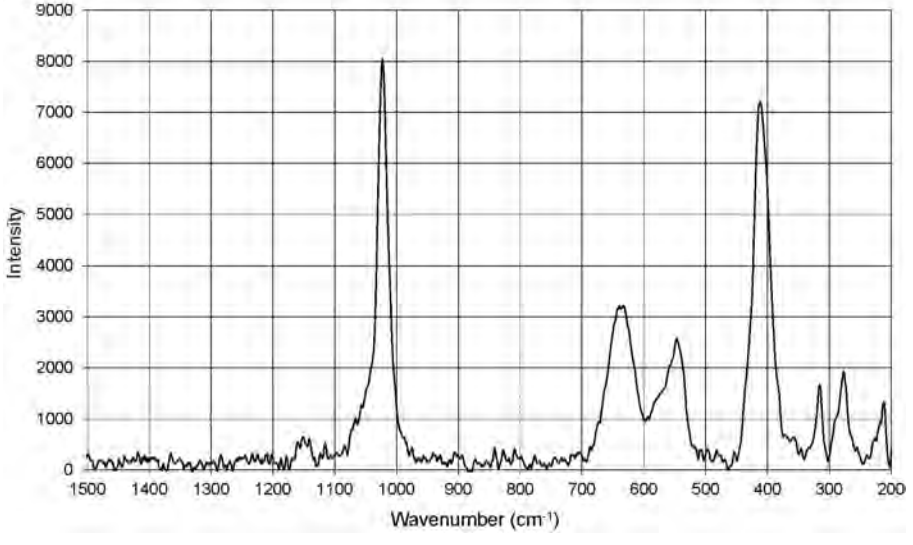
9000
8000
7000
6000
5000
4000
3000
2000
1000
0
Intensity
1500
1400
1300
1200
1100
1000
900
800
700
600
500
400
300
200
Wavenumber (cm-1)

Figure 5

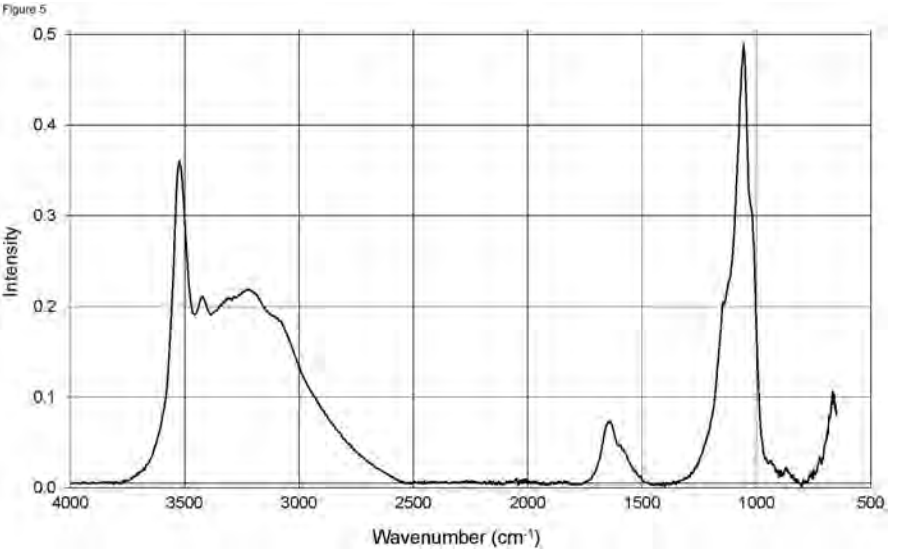
0.5
0.4
0.3
0.2
0.1
0.0
Intensity
4000
3500
3000
2500
2000
1500
1000
500
Wavenumber (cm-1)

Figure 6

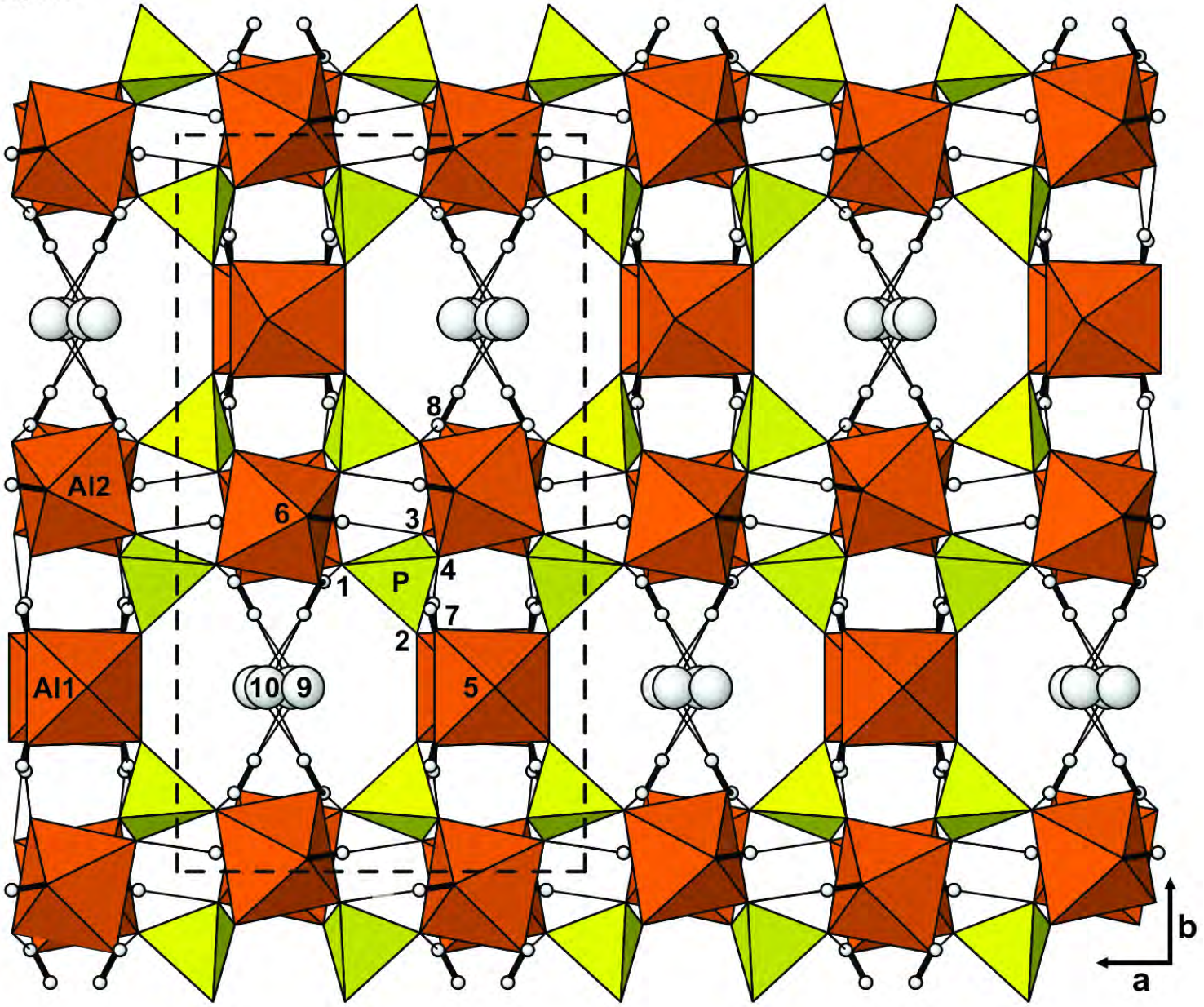

Figure 7